

# Links between magnetron plasma spokes and short-scale electron density fluctuations: insights from *pseudo 3D* particle modelling and coherent Thomson scattering

Adrien Revel<sup>1</sup>, Sedina Tsikata<sup>2</sup>, Claudiu Costin<sup>3</sup>, and Tiberiu M. Minea<sup>1</sup>

<sup>1</sup>LPGP, UMR 8578: CNRS-Université Paris-Sud, 91405 Orsay, France

<sup>2</sup>ICARE, UPR 3021 CNRS, 1C Ave. de la Recherche Scientifique, 45071 Orléans, France~

<sup>33</sup>Iasi Plasma Advanced Research Center (IPARC), Faculty of Physics, Alexandru Ioan Cuza University of Iasi, Bd. Carol I nr. 11, 700506 Iași, Romania

The physics of the magnetron discharge, in either direct current or high power pulsed regimes, appears dominated by instabilities which have been identified in two principal directions: azimuthal, *i.e.*, in the same direction as the main electron ( $\mathbf{E} \times \mathbf{B}$ ) drift, and normal to the cathode. *Pseudo 3D* particle modelling and coherent Thomson scattering experiments have identified mm-scale electron density fluctuations in the MHz range which appear linked to the formation of rotating spokes at longer time-scales.

## 1. Introduction

Several classes of instabilities have been identified in magnetized plasma devices ranging from tokamaks and pinch machines to plasma thrusters and magnetrons [1]. The manner in which such instabilities influence the features of plasma discharges has been an area of active research for decades.

The novel high-power pulsed operation mode known as HiPIMS (High-Power Impulse Magnetron Sputtering) for magnetrons has led to an increase in interest in the nature of instabilities present in these sources. High-density plasma structures, called ‘spokes’, have been recently identified in magnetron plasmas, rotating around the magnetron axis following the racetrack of the target, especially in HiPIMS operation mode [2,3]. Such structures have also been identified in the conventional direct current (DC) magnetrons [4] and appear to be a feature common to magnetrons and a range of other plasma devices.

Many explanations have been advanced to account for the origin of spokes, involving ion impact on the target, the development of ionization waves, plasma instabilities, and the release of electron bursts from the cathode. However, comprehension of this and other phenomena present in magnetron plasmas remains poor, in part due to a lack of suitable numerical and experimental approaches.

This contribution focuses on the origin of these electron density fluctuations in magnetron discharges using self-consistent *pseudo-3D* plasma modelling in HiPIMS mode and the exploitation of a highly-sensitive coherent Thomson scattering diagnostic initially developed for Hall thruster investigations [5].

Both approaches provide new insights into the presence of short-scale instabilities in the magnetron plasma, particularly in the range of MHz frequencies.

## 2. Numerical Background

The modelling of magnetized plasma requires at least a two-dimensional (2D) treatment, since the magnetic field induces an anisotropy. In the case of the magnetron discharge, the complex structure of the magnetic trap makes the problem intrinsically 3D, due to the fact that most of these instabilities propagate azimuthally, in the  $\mathbf{E} \times \mathbf{B}$  drift direction [6].

The numerical approach used here takes into account the space charge effect in three dimensions, with Poisson’s equation solved three times in three orthogonal planes. The Particle-In-Cell (PIC) method [7] permits very good quantitative descriptions of HiPIMS plasma behaviour in 2D due to its self-consistency.

PIC modelling requires significant resources for a single run, even in 2D, in addition to stability constraints. To obtain 3D results within a reasonable time frame (in order to capture instabilities which are 3D phenomena), the model has been adapted, always self-consistently, with the third dimension included. However, the use of the PIC method in full 3D is not feasible because of the prohibitive memory and computation times involved. Instead, a *pseudo 3D* approach has been developed and successfully exploited.

This approach consists of moving all the macroparticles in the 3D volume with a periodic boundary condition in the azimuthal direction. Knowledge of the 3D electric field is necessary, and is

obtained in two steps (with reference to a coordinate system where  $x$  is axial,  $z$  radial and  $y$  azimuthal):

(i) first, a full 2D PIC simulation is performed in one plane, normal to the cathode and containing the magnetic field lines, *e.g.*, the  $(x,z)$  plane leading to the electric field distribution in this plane  $(E_x, E_z)$ . The particles are all projected onto this plane and the component of the electric field in the  $y$ -direction is not considered at this stage of the model.

(ii) second, a 2D PIC simulation is performed assuming the  $(E_x, E_z)$  distribution known from the previous step, with the macroparticles projected on the other two orthogonal planes, namely  $(x,y)$  and  $(y,z)$ , to give  $E_y(x,y)$  and  $E_y(y,z)$ . Hence  $E_y$  can be estimated in any point of the volume from  $E_y(x,y,z) = 0.5(E_y(x,y) + E_y(y,z))$ . The movement of the particles in the  $x$ - and  $z$ -directions is calculated with the electric field obtained in (i) (*i.e.*,  $E_x$  and  $E_z$ ).

Hence, all the field components are known at any location in the 3D simulation volume and the computational time is considerably reduced. This approach permits a good qualitative description of particle trajectories in 3D. It has been coupled with a Monte Carlo Collision (MCC) treatment using a null collision technique. Details on the MCC treatment can be found in [7].

### 3. Experimental diagnostic

The collective Thomson scattering experiment was performed on a magnetron argon plasma with a planar 10 cm-diameter titanium target. Two different operation regimes, DC and HiPIMS, were studied. More details on the source and chamber can be found in [8].

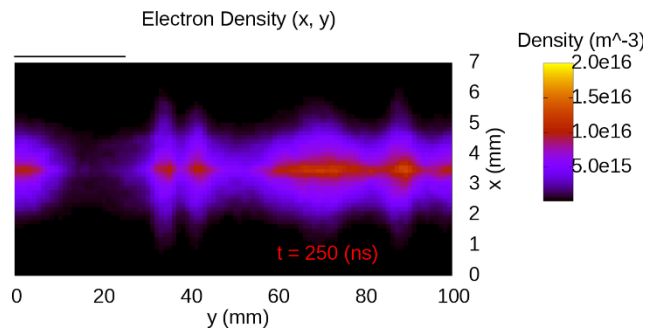
The diagnostic, PRAXIS, measures correlated fluctuations of electron density via Thomson scattering, at set length scales and wave vector orientations. Optical access to the plasma in the vicinity of the cathode is provided via IR-transparent ZnSe windows on the vacuum vessel. The diagnostic uses a CO<sub>2</sub>, 10.6  $\mu\text{m}$ -wavelength laser beam, split into primary and local oscillator components, for scattering and for the definition of the wave vector properties. The beams intersect in the plasma region of interest in front of the cathode, defining the observation volume [8].

In this implementation, electron density fluctuations are measured at short-scales ( $\sim 1$  mm length scales and below, on the order of the electron Larmor radius). At these scales, the diagnostic has been successfully used to identify and characterize the MHz electron cyclotron drift instability in Hall thrusters [10].

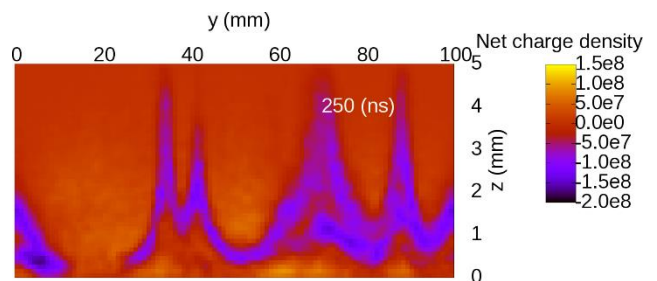
### 4. Results and discussion

Numerical simulations (Figs. 1 and 2) show that the velocity drift  $\mathbf{ExB/B}^2$ , combined with the space charge repulsion, leads to sharp non-uniformities of the electron density in the magnetron plasma along the azimuthal direction.

Indeed, despite the uniform plasma distribution along the azimuthal direction ( $Oy$ ) at the beginning of the simulation, after only a few tens of ns the electron density creates self-organized structures of very high density (red region – Fig. 1). These structures are separated by regions of very low electron density (black – Fig. 1). Note that the coefficient of secondary electron emission from the cathode is constant and uniform over the entire cathode surface and for the entire simulation duration.

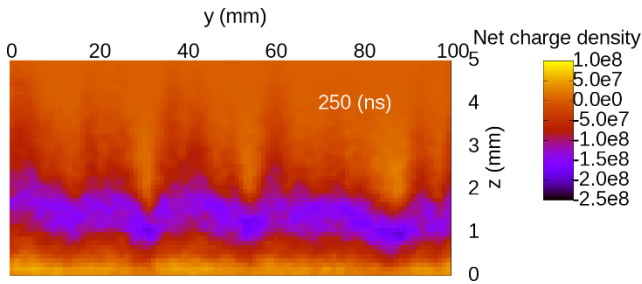


**Figure 1.** Top view of the electron density projected onto the cathode plane after 250 ns, obtained by *pseudo-3D* PIC modelling in HiPIMS mode, with  $I_{\text{max}} = 10\text{A}$  and  $V_{\text{cath}} = -600\text{V}$ ,  $P=0.4$  Pa.



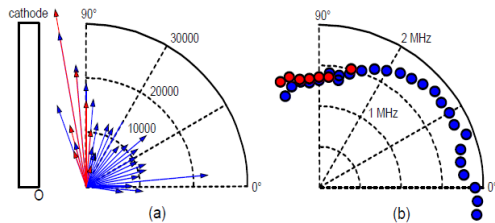
**Figure 2.** Side view of the net charge density projected onto the plane along the racetrack perpendicular to the cathode after 250 ns, in HiPIMS mode, with  $I_{\text{max}} = 10\text{A}$  and  $U_{\text{cath}} = -600\text{V}$ ,  $P=0.4$  Pa.

Figure 2 shows the projection of the net charge density along the  $y$ -axis (horizontal axis), but perpendicular to the target, at the same moment as in Fig. 1. Over-dense regions occupied by the ions (orange) very close to the target are visible, and the electrons are observed to escape mainly in the  $z$ -direction, normal to the cathode, leading to flare formation, as experimentally observed by Anders and colleagues using fast (ns) cameras [2].



**Figure 3.** Side view of the net charge density projected onto the plane along the racetrack perpendicular to the cathode after 250 ns, in DC mode with  $I = 1\text{ A}$  and  $U_{\text{cath}} = -300\text{ V}$ ,  $P = 0.4\text{ Pa}$ .

When the discharge current is decreased from 10A (HiPIMS) to 1A (DC - Fig. 3), the side-view of the net charge density along the  $y$ -axis does not show significant separation, with only a modulation at a certain distance from the cathode visible. The positive charge (orange) dominates close to the target, while the negative charge (purple) dominates for larger  $z$ . Again, electrons appear to escape from the magnetic trap mostly normal to the cathode and flowing small spikes.



**Figure 4.** Collective Thomson scattering results showing the variation in (a) mode amplitude and (b) frequency as a function of orientation angle in the  $(\mathbf{E}, \mathbf{E} \times \mathbf{B})$  plane.  $O$  represents the center of the cathode. DC operation:  $U_{\text{cath}} = 370\text{ V}$ ,  $I = 0.4\text{ A}$ ; observation wavenumber  $k = 5600\text{ rad/m}$ .

Interestingly, coherent Thomson scattering investigations identify similar behaviour of the electron density fluctuations: a sharp peak in the amplitude of electron density fluctuations close to the direction normal to the cathode surface (Fig. 4a). At  $5^\circ$ , the mode amplitude jumps to a value twice found that observed at neighbouring angles.

For the same HiPIMS discharge condition (10A), Figure 5 shows the simulation results for the instantaneous ion density (top) and the electron density integrated over  $1\ \mu\text{s}$  (bottom). These results seem to be coherent with the experimental observation of a homogenous plasma for long exposure times of the camera, as found by Anders *et al.* [2] (Fig. 6).

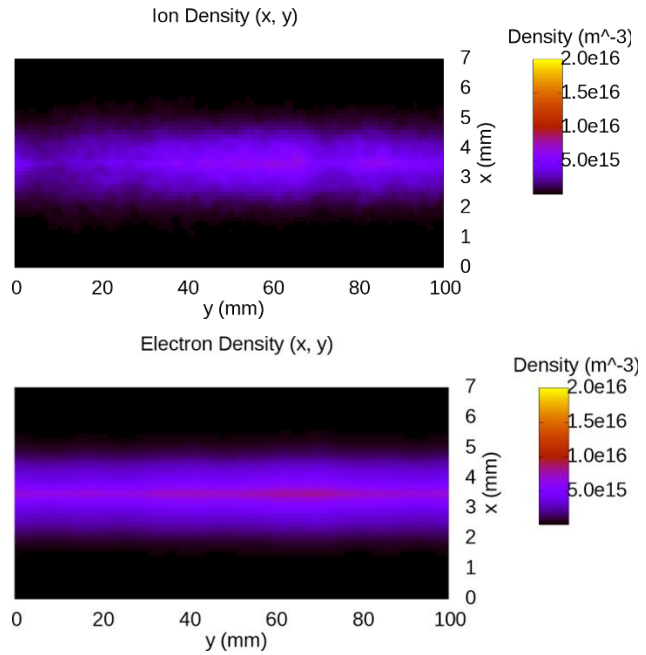


**Figure 5.** Top view of the instantaneous ion density (top) after 250 ns, and the total electron density integrated during  $1\ \mu\text{s}$  (bottom), projected onto the cathode plane after 250 ns, obtained by *pseudo-3D* PIC modelling in HiPIMS with  $I_{\text{max}} = 10\text{ A}$  and  $V_{\text{cath}} = -600\text{ V}$ ,  $P = 0.4\text{ Pa}$ .

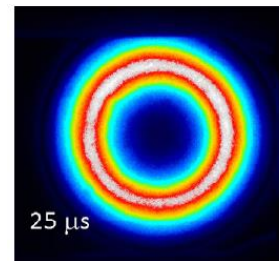


**Figure 6.** Top view of the light emission from the HiPIMS magnetron plasma recorded with an exposure gate of  $25\ \mu\text{s}$ , from [2].

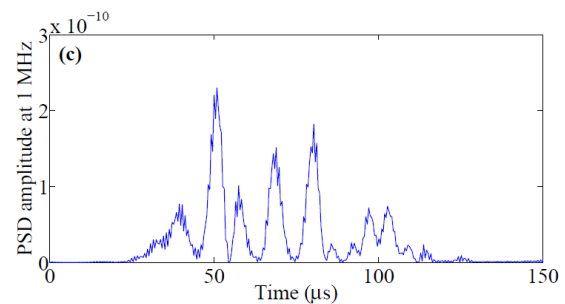


**Figure 7.** Thomson scattering signal showing the time evolution of power spectral density at  $1\text{ MHz}$ , showing low-frequency periodicity HiPIMS operation:  $U_{\text{cath}} = 494\text{ V}$ ,  $I = 7\text{ A}$ ;  $k = 5600\text{ rad/m}$ .

Further analysis of the Thomson scattering signal observed at a particular frequency (Fig. 7) may be performed. A spectrogram of the scattering signal is first determined, and the power spectral density

amplitude at a fixed frequency of 1 MHz (within the frequency range where the mode has been identified to be present) is shown. The MHz instability shows a modulation at a much lower frequency (~120 kHz), which is compatible with characteristic spoke characteristic frequency reported by other authors [2-4].

Experimental and modelling results appear to support the notion that drift instabilities (specifically, of the short-scale electron cyclotron type identified in experiments) may exhibit a low frequency modulation. Plasma spokes seem to be large-scale phenomena which may be generated by short-scale instabilities of the type observed in this work, consistent with the explanations advanced by Brenning *et al* [6].

## 5. Concluding remarks

Two independent approaches, one based on the *pseudo-3D* PIC Modelling and the other exploiting the coherent Thomson scattering, have been used to characterize the plasma instabilities in magnetron discharges. In DC or HiPIMS operation modes, a short-scale MHz drift instability (identified as the electron cyclotron drift instability) is consistently present.

Simulation results are in good qualitative agreement with measurements, with both showing that plasma electrons escape from the magnetic trap normal to the cathode.

Low frequency modulation of the MHz instabilities is apparent from coherent Thomson scattering experiments, at time scales which are compatible with the characteristic rotation times of spokes.

These results provide insights into the possible mechanisms of spoke formation and propagation in magnetron discharges.

## Acknowledgement

This work was partially supported by the *Pôle d'Attraction Interuniversitaire* (PAI, P7/34, 'Plasma-surface interaction', Belgium) and the *Réseau Plasmas Froids* (France).

## References

- [1] Francis F. Chen, Introduction to Plasma Physics, Springer US, (2012)
- [2] A. Anders, P. Ni, and A. Rauch, J. Appl. Phys. 111, 053304 (2012).
- [3] A. P. Ehiasarian, A. Hecimovic, T. de los Arcos, R. New, V. Schulz von der Gathen, M. Böke, and J. Winter, Appl. Phys. Lett. 100, 114101 (2012)
- [4] J. Winter, A. Hecimovic, T. de los Arcos, M. Boke, and V. Schulz von der Gathen, J. Phys. D: Appl. Phys. 46, 084007 (2013)
- [5] J. Cavalier, N. Lemoine, G. Bonhomme, S. Tsikata, C. Honoré, and D. Grésillon, Phys. Plasmas 20, 082107 (2013).
- [6] N. Brenning, D. Lundin, T. Minea, C. Costin, and C. Vitelaru, J. Phys. D: Appl. Phys, **46** (2013) 084005
- [7] T. Minea, C. Costin, A. Revel, D. Lundin, L. Caillault, Surf. Coat. & Technol. Volume(s) 255, 52 (2014)
- [8] C. Vitelaru, L. de Poucques, T. M. Minea, and G. Popa, J. Appl. Phys. 109, 053307 (2011).
- [9] S. Tsikata, N. Lemoine, V. Pisarev, and D. Grésillon, Phys. Plasmas 16, 033506 (2009)
- [10] S. Tsikata, J. Cavalier, A. Héron, C. Honoré, N. Lemoine, D. Grésillon, and D. Coulette, Phys. Plasmas 21, 072116 (2014)